

Division - Soil in Space and Time | Commission - Soil Genesis and Morphology

Micromorphology and Genesis of Soils from Topolitosequences in the Brazilian Central Plateau

Fernando Cartaxo Rolim Neto^{(1)*} , **Carlos Ernesto Gonçalves Reynaud Schaefer⁽²⁾** , **Danilo de Lima Camêlo⁽³⁾** , **Marcelo Metri Corrêa⁽⁴⁾** , **Roberto da Boa Viagem Parahyba⁽⁵⁾** , **Anildo Monteiro Caldas⁽¹⁾**  and **Anifo Soares Mamudo Ibraimo⁽²⁾** 

⁽¹⁾ Universidade Federal Rural de Pernambuco, Departamento de Tecnologia Rural, Recife, Pernambuco, Brasil.

⁽²⁾ Universidade Federal de Viçosa, Departamento de Solos, Viçosa, Minas Gerais, Brasil.

⁽³⁾ Universidade Federal do Espírito Santo, Departamento de Agronomia, Alegre, Espírito Santo, Brasil.

⁽⁴⁾ Universidade Federal Rural de Pernambuco, Unidade Acadêmica de Garanhuns, Garanhuns, Pernambuco, Brasil.

⁽⁵⁾ Empresa Brasileira de Pesquisa Agropecuária, Embrapa Solos, Recife, Pernambuco, Brasil.

ABSTRACT: The micromorphology of deeply weathered soils (Ferralsols/*Latossolos*) from the Central Plateau of Brazil remains little studied, and its affiliation to different parent materials, poorly known. To clarify the processes of soil formation of these acric, gibbsitic, Fe-oxide rich Ferralsols, three lithotoposequences on local ultrabasic to basic intrusive rocks were studied. The influences of mixing and pedobioturbation are evident in all soils, and Ferralsols of the Central Plateau of Brazil are polygenetic, based on the coarse mineral composition, with ultrabasic and metapelitic rock contributions. The typical oxic microstructure with stable microaggregates encompasses a gibbsite/Fe rich micromass with random inclusions of charcoal, allochthonous quartz, Ti-magnetite, and perovskite grains. Shallow Cambisols (*Cambissolos*) on tuffites also display a similar “oxic” microstructure, but a much lower degree of weathering. These Cambisols possesses apatite, and mafic and pelitic minerals as residuals minerals grains, indicating the polygenetic colluvia mixture of different substrates. The common occurrence of perovskite (CaTiO₃) as a residual grain in deep-weathered, acric Ferralsols on ultrabasic rocks, not yet reported in the literature, shows an unusual resistant Ca reserve in oxic soils, though nothing is known about its implications to soil fertility.

Keywords: Ferralsols, Cambisols, mafic rocks, ultramafics, perovskite, tropical soils.

*** Corresponding author:**

E-mail: fernandocartaxo@yahoo.com.br

Received: October 24, 2018

Approved: June 19, 2019

How to cite: Rolim Neto FC, Schaefer CEGR, Camêlo DL, Corrêa MM, Parahyba RBV, Caldas AM, Ibraimo ASM.

Micromorphology and genesis of soils from topolitosequences in the Brazilian Central Plateau. Rev Bras Cienc Solo. 2019;43:e0180219.

<https://doi.org/10.1590/18069657rbcsc20180219>

Copyright: This is an open-access article distributed under the terms of the Creative Commons Attribution License, which permits unrestricted use, distribution, and reproduction in any medium, provided that the original author and source are credited.



INTRODUCTION

The most weathered and oxic tropical soils are polygenetic, and formed from pre-weathered materials (Tardy and Roquin, 1992; Stoops et al., 1993; Thomas, 1994; Baert and van Ranst, 1997; Schaefer, 2001; Marcelino et al., 2018). They were subjected to cumulative, long-term ferralitization, pedobioturbation, and eventually, other soil-forming processes that led to great Bw horizon development, possessing peculiar micromorphological properties when compared to the soils from temperate regions (Schaefer, 2001). These soil are classified as Oxisols (Soil Survey Staff, 1999), *Latosolos* (Brazilian Soil Classification System; Santos et al., 2018) or Ferralsols (World Reference Base; IUSS, 2015), and their physical and structural properties are very favorable for root development (Ker, 1997), despite the very low fertility status. The widespread distribution and agricultural importance of such soils make micromorphological studies important for the understanding of their genesis, use, and management.

Compared to other soil orders, little detailed work has been undertaken on the microstructural and microchemical properties of Ferralsols (Stoops and Buol, 1985; Schaefer et al., 2002; Paisani et al., 2013), despite being required to support genetic and taxonomical studies. Previous studies, such as Miklós (1992), Duarte et al. (1996), Muggler and Buurman (1997), Marques (2000), Nunes et al. (2000), Schaefer (2001), Paisani et al. (2013), and Stoops and Schaefer (2018) have assembled important data on the micropedology of Ferralsols, relating the micropedological features observed with other aspects, such as pedogenesis, geomorphological evolution of the landscape, chemistry and soil fertility, among others.

The Brazilian Central Plateau represents the largest agricultural frontier in the tropics (Cerrado region), and some studies have focused on micromorphological aspects of the main regional soils, especially those developed from basalt, sandstone, and Late Tertiary sedimentary covers (Marques, 2000). However, little is known about the micromorphological and microchemical properties of Ferralsols or Cambisols developed from mafic to ultramafic igneous/alkaline volcanic province of the Upper Paranaíba headwaters (Barbosa et al., 1970), although several studies have examined detailed mineralogy of these soils (Carmo et al., 1984; Ferreira et al., 1994; Rolim Neto et al., 2009; Camêlo et al., 2017, 2018).

This study aimed to evaluate the micromorphological properties, at both optical and scanning electron microscopy scales, coupled with wavelength and energy dispersive X-ray spectroscopy for microchemical elemental composition and mapping, to enhance the knowledge of such deep weathered highland soils with reference to the genesis implications.

MATERIALS AND METHODS

Seven soil profiles were selected in three topolithosequences located in the Upper Paranaíba Plateau in the state of Minas Gerais, between the cities of Serra do Salitre (topolithosequence 1), Patrocínio (topolithosequence 2), and Coromandel (topolithosequence 3) (Figure 1), across the geological contact zone between the Bambuí and Araxá Groups, where volcanic materials outcrop as lava or plugs. Cross-sections of the studied topolithosequences are presented by Rolim Neto et al. (2009).

The regional climate is subtropical Cwb (Köppen Climate Classification System), with mild summers and dry winters (Alvares et al., 2013). The soil classification, geology, geomorphology, and vegetation are presented in table 1.

For the micromorphological studies, samples of selected soil horizons were collected in aluminum boxes, oven-dried at 35 °C, and then impregnated with polyester resin at room temperature. Thin sections (4 × 10 cm) were produced and studied by a petrological microscope (optical microscopy) to describe the main micropedological

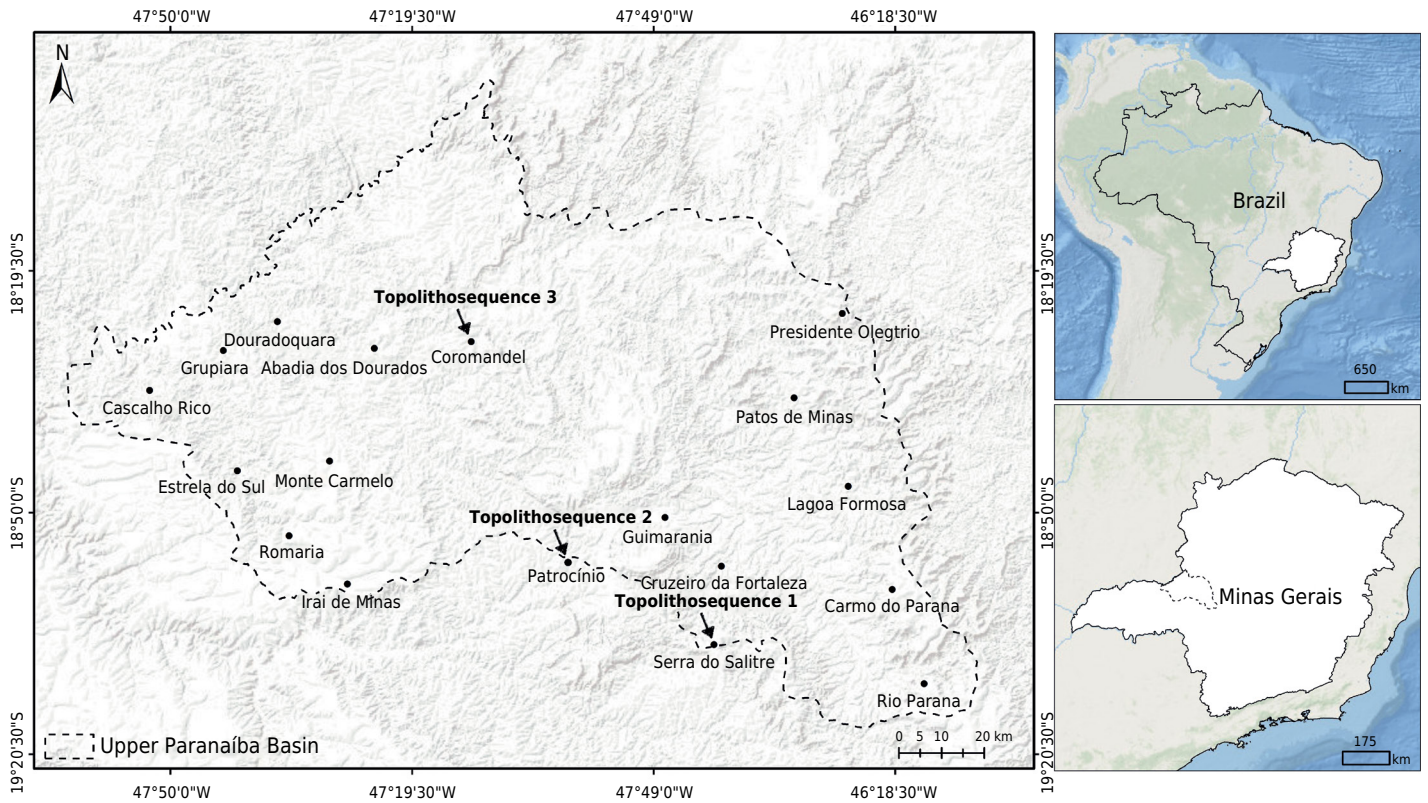


Figure 1. Location of the studied topolithosequences in the Upper Paranaíba Basin.

features, according to the methods described by Bullock et al. (1985), Stoops (2003), and Stoops et al. (2018). Propositions of Delvigne (1998) were also used to describe the alteration of mineral grains present. The terminology was based on the proposals of the International Union of Soil Sciences (IUSS) Handbook (Bullock et al., 1985), with adaptations of Stoops et al. (2018). Minerals in the fine sand fraction were further identified through a binocular microscope.

Selected thin sections were ultra-polished with 1 μm diamond paste, ultrasonic washed, and were coated with a conductive carbon film, to be examined and photographed in a scanning electron microscope, model JEOL JSM 6400, with a wavelength-dispersive X-ray spectrometer (SEM-WDS) for microchemical analysis of selected features. Each point-source microchemical analysis was performed with three replicates, with a voltage of 15 kV, 5 A, and 39 mm work distance (detector-surface), with recalibration after each analytical procedure. Microchemical maps for major elements (Si, Al, Fe, Ti, Mn, Ca, Mg, and P) and some trace elements were also obtained for selected areas by energy dispersive spectroscopy (SEM-EDS). After, preliminary identification of micropedological features by the microchemical maps, point-source analyses of these features were proceeded at high magnification. All micropedological features were recorded by backscattered electron (BSE) images to visualize their morphology.

RESULTS

Serra do Salitre topolithosequence

At the upland Acric Rhodic Ferritic Ferralsol ($P_1 - Bw_2$), a small granular microstructure is strongly developed, with abundant biological channels filled with pelletized materials (Figure 2a). Microfragments of charcoal are common within aggregates, as well as quartz grains, opaque minerals (magnetite), and gibbsite-hematite nodules (Table 2).

Table 1. Soil classification, geology, geomorphology, and vegetation of the three topolithosequences

Profiles	Soil Classification ⁽¹⁾	Geology	Geomorphology	Vegetation
Serra do Salitre topolithosequence				
P ₁	Acric Rhodic Ferritic Ferralsol (Clayic, Dystric)	Coverage derived from alkaline rock (igneous)	High flattened surface (plateau)	Degraded pasture
P ₂	Eutric Chromic Leptic Cambisol (Humic, Loamic)	Alkaline rock (igneous)	Dissected edge	Degraded pasture
P ₃	Geric Acric Rhodic Ferralsol (Clayic, Dystric)	Aluminous phyllite and chlorite-schists, Pre-Cambrian (BambuÍ)	Lower surface flush	Degraded pasture
Patrocínio topolithosequence				
P ₄	Geric Acric Gibbsic Ferralsol (Clayic, Dystric)	Coverage derived from ultramafic rock (peridotite/dunite)	Depression within the plateau	Coffee/successional vegetation
P ₅	Acric Rhodic Ferritic Ferralsol (Clayic, Dystric, Humic)	Precambrian metasedimentary rock (Araxá)	Lower surface flush	Secondary forest
Coromandel topolithosequence				
P ₆	Eutric Chromic Petroplinthic Leptic Cambisol (Clayic, Humic)	Volcanic tuffs of the Mata da Corda Formation (Mesozoic)	Dissected slopes of the plateau	Low successional vegetation
P ₇	Geric Rhodic Petroplinthic Ferralsol (Clayic, Dystric)	Lateritic materials covering colluvium of the plateau	Dissected lower surface	Low successional vegetation/Savannah

⁽¹⁾ According to IUSS Working Group WRB (2014).

In the A horizon of the Eutric Chromic Leptic Cambisol (P₂) of Serra do Salitre, a strong subrounded granular structure is present, containing abundant grains of nutrient-rich primary minerals, such as K and Mg-rich micaceous fragments (Figure 3a), intergrowth Ti-magnetite (Figure 3b), and intergrowth perovskite/ilmenite grains within larger aggregates (Figure 3c). Microchemical analyses confirm the ultramafic/alkaline nature of the Serra do Salitre soils, in which the micromass composition is rich in 2:1 clay minerals (Rolim Neto et al., 2009), with high, but varying amounts of P, K, Mg, and Ti. Beside K, the presence of Ca/Mg minerals highlights the high nutrient reserve of the Cambisol.

In the P₂, developed “in situ” from alkaline-ultrabasic rocks, the Bi horizon showed an unusual well-developed microgranular structure (Figure 2b), containing abundant primary minerals, mainly quartz, degraded micaceous grains, hornblende (not shown), and apatite grains (Figure 4a), all mixed with charcoal fragments (Figure 2c).

The micromass is locally dark, due to organic-matter impregnation, with anisotropic, striated zones, where primary minerals inclusions occur within aggregates. Intense biological activity is evidenced by abundant fecal pellets, with little presence of humified organic remains (Table 2; Figure 2d). Besides the microgranular structure (Figure 2b), in Bi horizon several Mg/K rich grains of micaceous nature occur (Figure 3a), Ti-magnetite inclusions (Figure 3b), associated with trace elements and abundant perovskite grains, some of which intergrowth with Ti-magnetite (Figure 3c), as also illustrated for A horizon. The well-developed granular structure detected

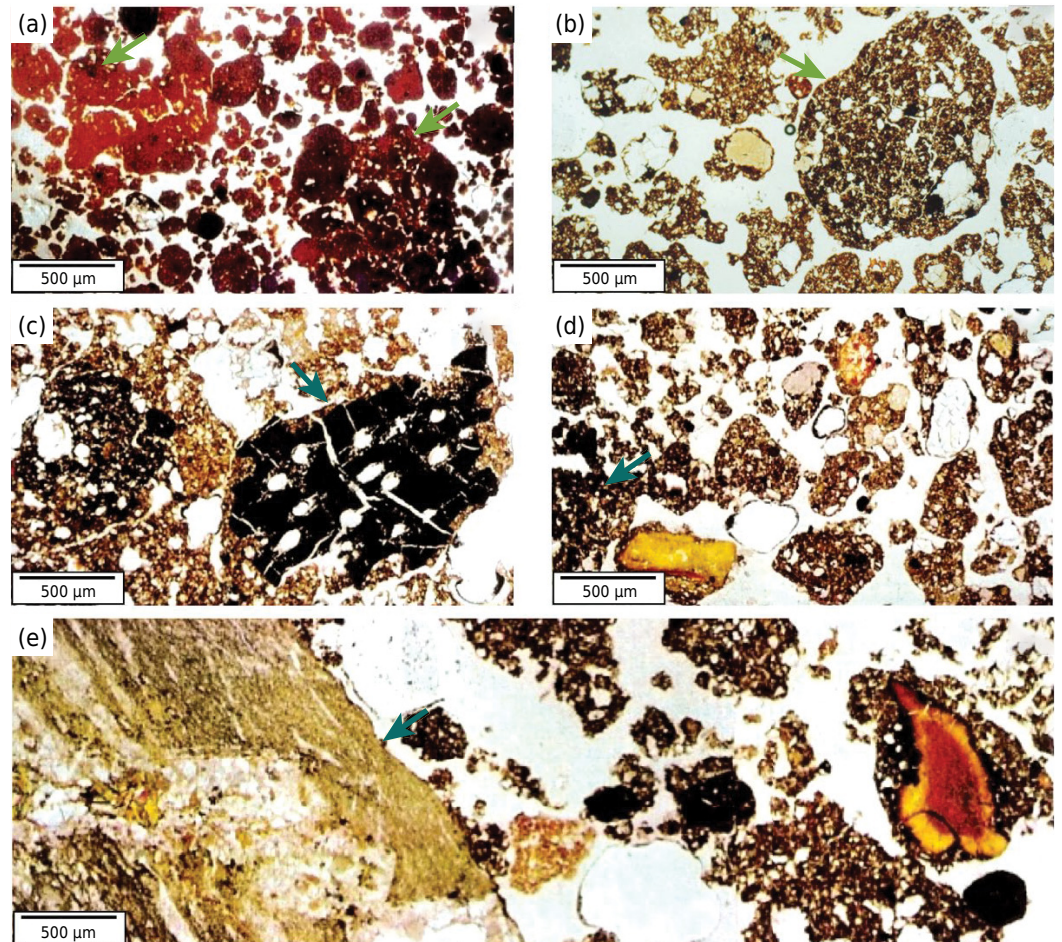


Figure 2. Photomicrographs of the Bw_2 horizon (a) in the P_1 - Acric Rhodic Ferritic Ferralsol (Clayic, Dystric) and of the Bi horizon (b, c, d, and e) in the P_2 - Eutric Chromic Leptic Cambisol (Humic, Loamic); Serra do Salitre topolithosequence. Arrows indicate pelletized materials filling and charcoal microfragments (a), well-developed microgranular structure in the cambic horizon (b), charcoal fragment (c), humified organic remains (d), and fragments from acid metapelitic rocks mixed with altered and pedoplasmated material of volcanic origin (e).

macroscopically for cambic horizon, atypical for Cambisols, was evident in backscatter photomicrographs obtained by SEM (Figures 4b and 4c).

In terms of chemical composition, the most common coarse fragments (Figure 2e), have high amounts of Fe, K, Mg, and low Ca (Figure 4b), representing fragments from acid metapelitic rocks belonging to the Bambuí Group, mixed with altered and pedoplasmated material of volcanic origin. The presence of micro-quartz veins in fragments, as described by optical microscopy, was confirmed by SEM analysis from the Si mapping (Figure 4b).

Degraded apatite grains observed under optical microscopy and SEM are scattered within microaggregates of the Bi horizon (Figure 4a). Microchemical analyses of these corroded grains indicate high contents of P_2O_5 (up to 18.10 %) in the preserved core, decreasing to 12.70 % P_2O_5 on the edge, where Fe impregnation occurs (Table 3; Figure 4a). However, the surrounding micromass is P-depleted. The degradation of these grains is confirmed by the replacement of Ca for Al, with much lower values of Ca (4.10-4.30 % CaO) relative to Al.

In the Geric Acric Rhodic Ferralsol (P_3), the Ap horizon showed a strongly coalesced granular structure (Figure 5a), forming subangular blocks (Table 2). The BA horizon shows a typical oxic microstructure (Figure 5b), with larger aggregates compared

Table 2. Micropedological features of the selected horizons of soils in the Serra do Salitre topolithosequence

Samples	Microstructure ⁽¹⁾	Pores ⁽²⁾	Grains	Micromass ⁽³⁾	Organic material	Associated structures
P ₁ - Bw ₂	Strong microgranular	40 %; intergranular and biological channels	Common grains of quartz and titanium; opaque micronodules of Gb and Hm	Isotropic; reddish brown and dark brownish red	Microaggregates with biological origin; fecal pellets; rare roots; common charcoal fragments	Micronodules; Ti opaque minerals
P ₂ - Bi	Comprised in microgranular and subangular blocky	40 %; intergranular and biological channels and, rare flattened pores	Lithorelics of metapelitic, quartz, amphiboles and micas degraded; ferruginous concretions; fragments of volcanic rocks; opaque various	Isotropic part with anisotropic ridged areas interaggregated, by the presence of micaceous minerals; dominantly dark reddish brown in parts	Microaggregates of biological origin; fecal pellets; roots and abundant coals	Micronodules and ferruginization of gravels and primary grains; residual grains of apatite, mica, and titanium with ferruginization
P ₃ - Ap and BA	Composed in microgranular and subangular on the Ap; microgranular on the BA	35 % on the Ap; intergranular channels, cavities, flattened pores; 50 % on the BA	Sesquioxide nodules, common grains of quartz and titanium on the Ap and BA	Isotropic on the Ap and BA; reddish brown and brownish yellow on the Ap and dark brownish red on the BA	Leftovers of roots; coalesced microaggregates; fecal pellets and coals	Degraded micronodules
P ₃ - Bw ₂	Strong microgranular, dominantly between 150 and 500 µm	50 %; intergranular channels and biopores	Grains of quartz and titanium; sesquioxide nodules	Isotropic; reddish brown and dark red	Microaggregates of biological origin; rare roots; biological filled channels	Degraded micronodules
P ₃ - Bw ₃	Microgranular with massiveness in parts; dominantly <150 µm	45 %; intergranular channels and biopores	Edged grains of quartz, titanium and rare sesquioxide nodules	Isotropic, with areas with some anisotropy, by padding with dispersed clay	Microaggregates of biological origin; rare roots; biological filled channels	Degraded micronodules

⁽¹⁾ Type and degree. ⁽²⁾ Quantity and type. ⁽³⁾ Type and color. Gb: gibbsite; Hm: hematite.

with the underlying Bw₂ (Figure 5c). For the Bw₃ horizon, aggregates are significantly smaller (Figure 5d), with abundant oriented, striated clay plasma, as dispersed clay and biological channels (Figures 5d). Quartz grains (Figure 5d), Ti/Fe nodules (Figure 5c and Figure 6c) and microfragments of charcoal (Figures 5a and 5c) are randomly observed.

The well-developed oxic microstructure observed at greater scale (Figure 6a) shows subrounded quartz grains (Si map), ferruginous concretions (Fe map), and V-rich Ti-mineral grains (Ti and V maps). Point-source analyses of selected grains showed varying levels of Ti (Table 4), suggesting different degradation phases of ilmenite or rutile-ilmenite referred to as leucoxene (Jackson and Bates, 1997). It was observed a higher content of iron at the edges of these leucoxene grains (Fe maps), increasing their resistance to further weathering (Figure 6b, 6c, and 6d). The Ti-rich leucoxene phases are related to higher amounts of V and Nb, with low correlation with other Fe geochemically related elements (Cr and Mn) (Table 4). In the case of ferruginous concretions, microchemical maps revealed the association with Mn, Co, Cr, and Cu, but apparently without association with Ti (Figure 6e).

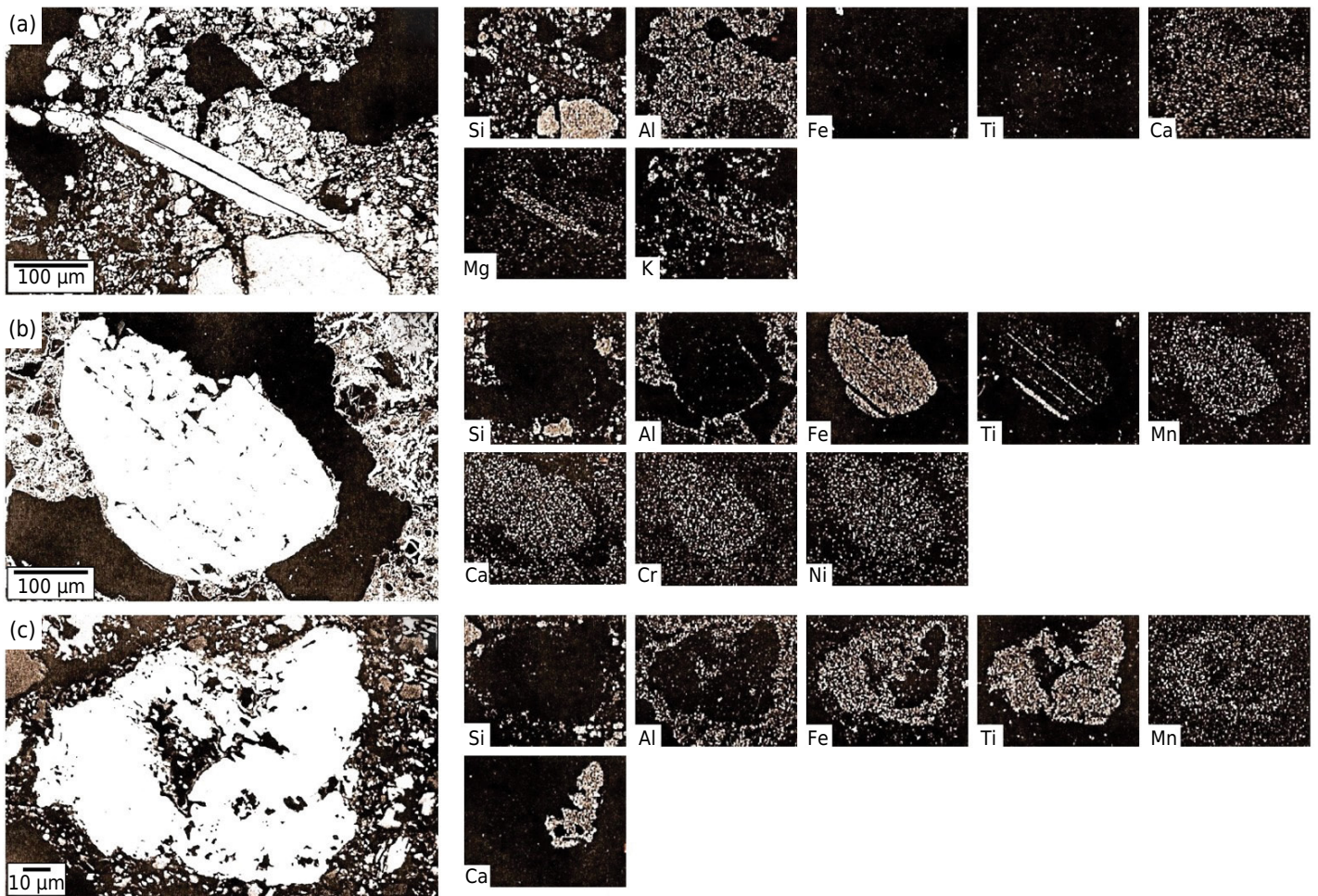


Figure 3. Scanning electron microscope photomicrographs and EDS microchemical maps of the A horizon in the P₂ - Eutric Chromic Leptic Cambisol (Humic, Loamic); Serra do Salitre topolithosequence. Abundant grains of K and Mg-rich micaceous fragments (a), intergrowth Ti-magnetite (b), and intergrowth perovskite/ilmenite grains within larger aggregates (c).

Patrocínio topolithosequence

At the highest landscape position, optical microscope observations of the Ap horizon of the upland Geric Acric Gibbsic Ferralsol (P₄) showed a bimodal pattern of aggregates (peaks >300 µm and <100 µm), with abundant porosity (Figure 7a). The underlying shows in the Bw₂ horizon, abundant biological channels in the strongly well-structured micromass, partially filled with welded aggregates, with quartz grains, Fe/Ti/Al nodules and unusual perovskite grains, randomly distributed in the matrix (Figure 7b).

The SEM backscattered images also illustrate a typical granular microstructure of the Bw₂ horizon of the P₄, with the scattered occurrence of Fe/Ti grains. The Fe/Cr-rich alteromorphs (Figure 8a) or Ti minerals occur as inclusions in the microaggregates (Figure 8b). The high variability in the chemical composition of these coarse grains indicates intense pedobioturbation and a polycyclic genesis of upland Ferralsols (Table 5).

For the Acric Rhodic Ferritic Ferralsol (P₅), the Ap horizon (not shown) showed larger aggregates compared with Bw₂ (Figures 7c and 7d), with frequent inclusions of rounded sand-sized quartz grains, Ti/Fe nodules, and perovskite grains. Common pedofeatures are biological channels with yellowish clay infillings and some dispersed clay between aggregates (Figures 7c and 7d). Microchemical observations of the Bw₂ in P₅ allowed identifying the unusual trace minerals assemblage with a marked signal of the ultramafic influence, suggesting a polygenetic nature. The microgranular structure is also typical

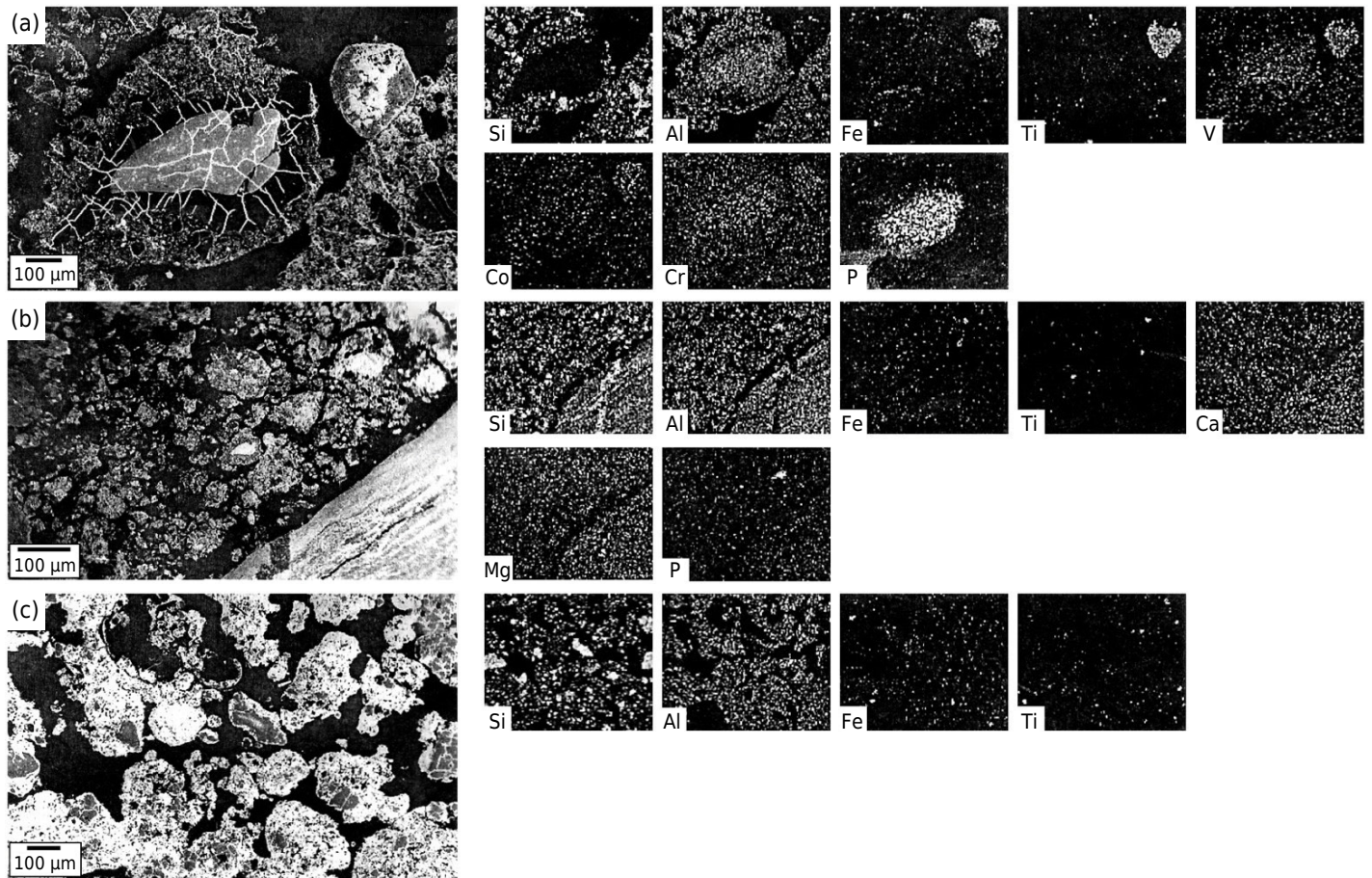


Figure 4. Scanning electron microscope photomicrographs and EDS microchemical maps of the Bi horizon in the P₂ - Eutric Chromic Leptic Cambisol (Humic, Loamic); Serra do Salitre topolithosequence. Degraded apatite grains within microaggregates (a), micro-quartz veins in lithorelict fragments (b), and quartz grains within a well-developed granular structure (c).

Table 3. The SEM-WDS microchemical analysis of selected pedofeatures of the Bi horizon in the P₂ - Eutric Chromic Leptic Cambisol (Humic, Loamic); Serra do Salitre topolithosequence

Oxide	Rock	P-nodule			Aggregate clay plasma
		Inner	Intermediary	External	
%					
MgO	3.20	0.66	0.52	0.40	2.50
Al ₂ O ₃	15.10	27.10	26.10	28.40	15.20
SiO ₂	37.20	5.10	6.20	36.60	25.40
P ₂ O ₅	0.16	18.10	12.70	0.26	0.40
K ₂ O	14.20	0.30	0.20	0.23	3.10
CaO	0.20	4.10	4.30	0.24	0.70
TiO ₂	1.61	5.20	2.10	0.28	2.80
CrO	0.04	n.d.	n.d.	0.20	0.20
MnO	n.d.	n.d.	n.d.	n.d.	0.10
Fe ₂ O ₃	8.20	8.80	12.80	8.40	13.30
CoO	n.d.	0.10	n.d.	0.14	n.d.
NiO	0.04	0.20	n.d.	n.d.	0.20
CuO	0.10	n.d.	n.d.	0.20	0.07
ZnO	0.30	0.36	n.d.	0.22	0.41
K _i ⁽¹⁾					2.84

⁽¹⁾ Weathering index (Ki) was only determined for micromass, in which $K_i = (SiO_2 \times 1.7)/Al_2O_3$; n.d.: not detected.

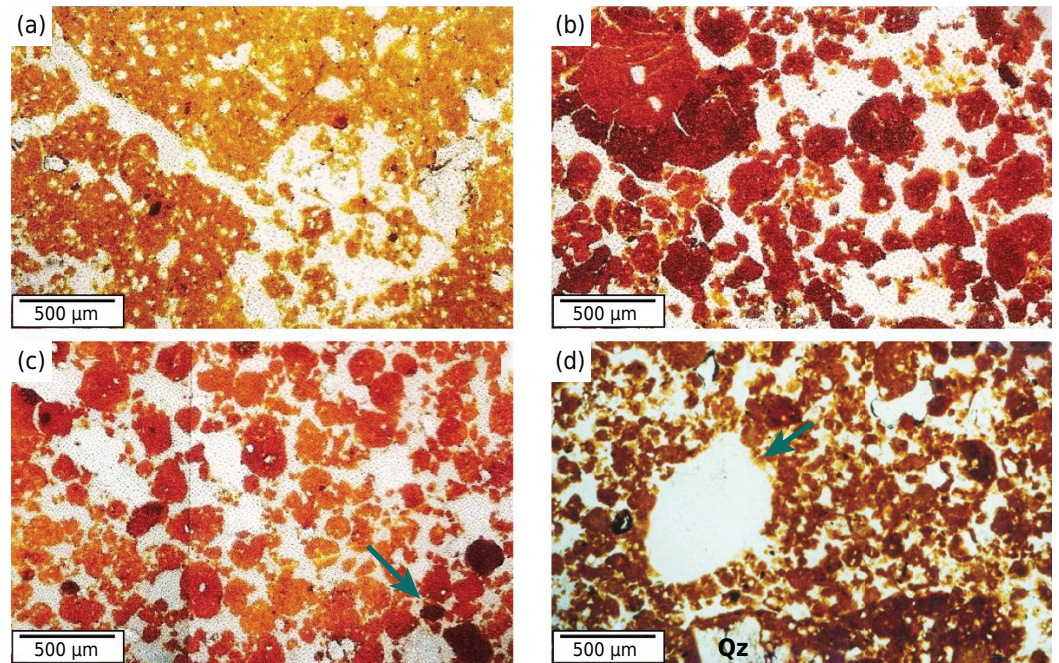


Figure 5. Photomicrographs of the Ap horizon (a), BA horizon (b), Bw₂ horizon (c), and Bw₃ horizon (d) in the P₃ - Geric Acric Rhodic Ferralsol (Clayic, Dystric); Serra do Salitre topolithosequence. Ap horizon showing a strongly coalesced granular structure (a), BA horizon showing a typical oxic microstructure (b), with larger aggregates compared with the underlying Bw₂ (the arrow shows a Ti/Fe nodule) (c), and for the Bw₃ horizon, aggregates are significantly smaller with abundant oriented, striated clay plasma, as dispersed clay and biological channels (arrow) (d). Qz: quartz.

of Ferralsols, with abundant Ti-rich alteromorphs (Figure 8c) and Ti/Fe opaque grains (Figure 8d) as observed by optical microscopy.

Microchemical analyses of these grains at point-source allowed the identification of perovskite (Ca, Ti, and Fe maps) (Figure 8c), a vitreous Ca-titanate (CaTiO₃) with high amounts of Ba and Nb (Table 6).

The perovskite grains are normally bordered by an external ferruginous feature (nodulation), which revealed a much lower Ca content by SEM-EDS analysis, and a Ti/Fe composition. In addition, titaniferous-ferruginous concretions formed by Ti-maghemite occur throughout, being derived from the alteration of primary Ti-magnetite, with low contents of Ca (Table 6).

The clay micromass is highly oxic (gibbsitic) with high Ti level, either as finely distributed anatase or Ti incorporated in the Fe oxides. This micromass is enriched with respect to Co and Ni (but not Cr), all trace elements normally associated with ultrabasic rocks. The clay infillings along biological channels show higher Ca and Mg values with a similar oxic composition (Table 6).

Individual or associated in aggregates, leucoxene grains (Ti/Fe) enriched in P and Nb (Table 6), are common (Figures 8c and 8d).

Coromandel topolithosequence

The Bi horizon in the Eutric Chromic Petroplintic Leptic Cambisol (P₆), showed a well-developed granular structure (Figure 9a), enriched with humified organic matter, fragments of volcanic ash with an ophitic texture, where mangans and ferrans are common along pores, and coating grains (Figures 9b and 9c). In the tuffite lithorelicts on unaltered magnetite grains (angular and opaque), occur in the greenish micromass of nontronite. Nontronite replaces pyroxene and mica crystals, while the large olivine

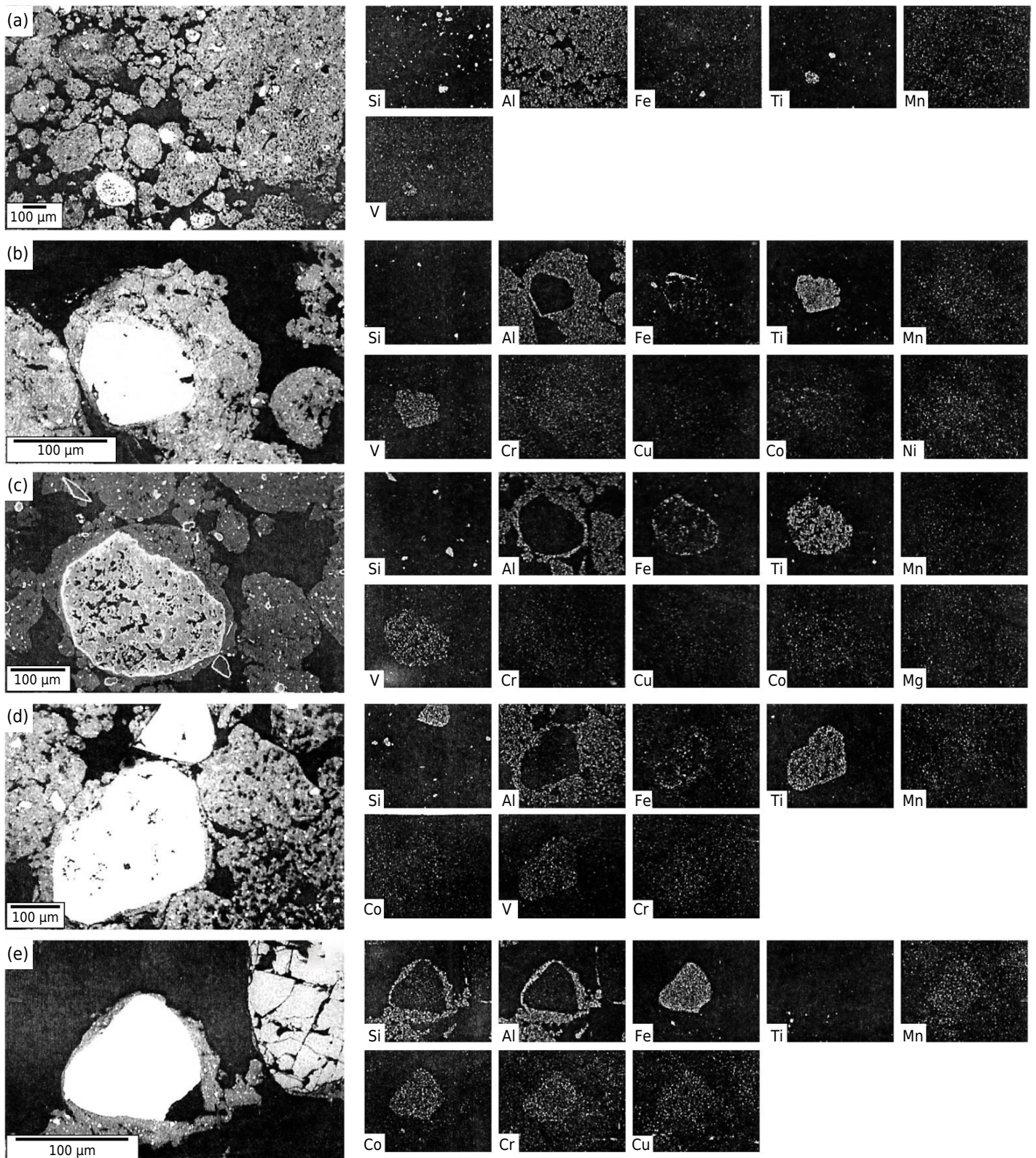


Figure 6. Scanning electron microscope photomicrographs and EDS microchemical maps of the Bw_2 horizon in the P_3 - Geric Acric Rhodic Ferralsol (Clayic, Dystric); Serra do Salitre topolithosequence. Well-developed oxic microstructure (a), a higher content of iron at the edges of the leucoxene grains (b, c, and d), and ferruginous concretions (e).

crystals are replaced by Fe-rich nontronite, forming dark masses in the tuffite fragments (Figures 9a and 9c). The microaggregates in the oxic micromass show an abrupt contact with these fragments; but transitional zones also occur, where gradual incorporation of fragmented tuffite (lithorelicts) is observed (Figure 9a).

Table 4. The SEM-WDS microchemical analysis of selected pedofeatures of the Bw₂ horizon in the P₃ - Geric Acric Rhodic Ferralsol (Clayic, Dystric); Serra do Salitre topolithosequence

Oxides	Ti-grain	Microaggregate clay plasma	Ti-grain		Ti-maghemite grain	Ti-grain	Aggregate plasma	Ferruginous concretion	Surrounding clay plasma
			Central	Margin					
%									
MgO	0.16	0.16	0.11	0.14	0.15	0.10	0.18	0.11	0.22
Al ₂ O ₃	0.10	30.20	0.32	0.31	1.51	0.45	30.5	3.40	29.30
SiO ₂	0.70	16.90	0.56	0.48	0.80	0.40	7.70	0.60	17.30
P ₂ O ₅	n.d.	0.36	0.30	0.70	1.10	0.26	0.16	0.10	0.21
K ₂ O	n.d.	n.d.	0.02	n.d.	n.d.	0.03	0.13	n.d.	0.12
CaO	0.14	0.03	0.07	0.13	n.d.	0.08	0.02	0.09	0.02
TiO ₂	57.00	4.10	55.20	50.70	41.00	51.4	3.13	0.40	2.60
CrO	n.d.	n.d.	0.03	0.02	0.35	0.25	0.08	0.30	0.18
MnO	n.d.	n.d.	n.d.	0.04	0.12	n.d.	n.d.	n.d.	n.d.
Fe ₂ O ₃	3.40	12.20	5.60	7.10	13.30	6.50	14.40	64.00	12.90
V ₂ O ₃	0.60	n.d.	0.30	0.03	0.38	0.50	n.d.	0.15	n.d.
NbO ₄	0.40	n.d.	0.60	0.55	n.d.	0.50	n.d.	n.d.	n.d.
Ki ⁽¹⁾		0.95					0.43		1.00

⁽¹⁾ Weathering index (Ki) was only determined for micromass, in which $Ki = (SiO_2 \times 1.7)/Al_2O_3$; n.d.: not detected.

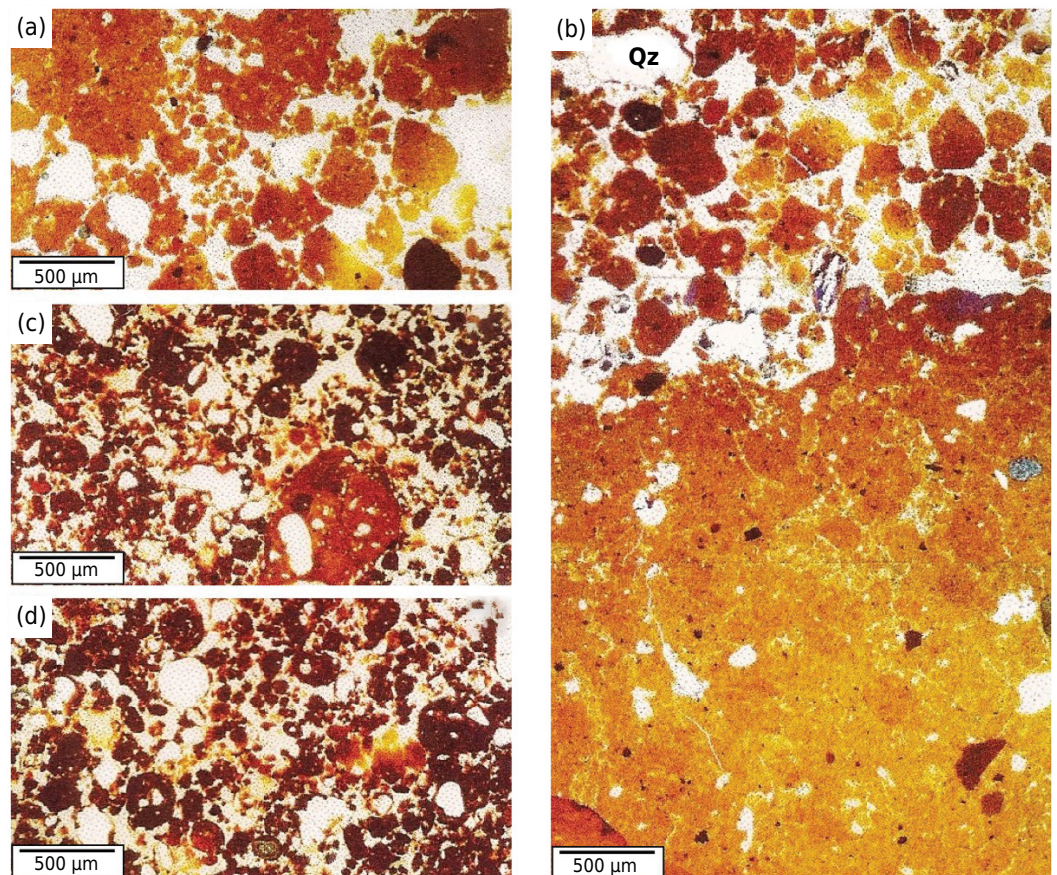


Figure 7. Photomicrographs of the Ap horizon (a) and Bw₂ horizon (b) in the P₄ - Geric Acric Gibbsic Ferralsol (Clayic, Dystric), and of Bw₂ horizon (c and d) in the P₅ - Acric Rhodic Ferritic Ferralsol (Clayic, Dystric, Humic); Patrocínio topolithosequence. Bimodal pattern of aggregates, with high porosity (a), abundant biological channels in the strongly well-structured micromass, partially filled with welded aggregates, with quartz grains, Fe/Ti/Al nodules and perovskite grains (b), and inclusions of rounded sand-sized quartz grains, Ti/Fe nodules, perovskite grains, biological channels with yellowish clay infillings and some dispersed clay between aggregates (c and d). Qz: quartz.

Table 5. The SEM-WDS microchemical analysis of selected pedofeatures of the Bw₂ horizon in the P₄ - Geric Acric Gbissic Ferralsol (Clayic, Dystric); Patrocínio topolithosequence

Oxides	Fe nodule (Cr-rich)	Ti-grain	Microaggregate clay plasma	Clay plasma surrounding Ti-grain	Aggregate clay plasma
%					
MgO	0.74	0.07	0.07	0.18	0.30
Al ₂ O ₃	2.85	0.16	32.20	31.70	33.40
SiO ₂	0.30	0.40	7.40	7.15	8.25
P ₂ O ₅	0.10	0.19	0.45	0.05	0.60
K ₂ O	n.d.	n.d.	n.d.	0.05	0.05
CaO	0.10	0.05	0.12	0.12	0.05
TiO ₂	0.80	52.80	4.10	2.95	4.25
Cr ₂ O ₃	7.10	0.10	0.32	0.30	0.25
MnO	0.20	0.02	0.06	n.d.	n.d.
Fe ₂ O ₃	55.70	6.20	18.30	17.90	17.30
CoO	0.20	0.20	0.28	n.d.	0.20
NiO	n.d.	0.05	0.23	n.d.	n.d.
CuO	n.d.	0.27	0.05	0.08	0.26
ZnO	n.d.	n.d.	n.d.	n.d.	n.d.
NbO	0.20	0.31	n.d.	0.20	0.12
Kj ⁽¹⁾			0.39	0.38	0.42

⁽¹⁾ Weathering index (Ki) was only determined for micromass, in which $Ki = (SiO_2 \times 1.7)/Al_2O_3$; n.d. = not detected.

Grains of perovskite and magnetite (not shown) are also dispersed both associated with lithorelicts, and in the oxic micromass. Hence, a rapid weathering and pedoplasation of these ultramafic tuffites under the current tropical climate are inferred forming well-structured soils, even at an incipient stage of pedogenesis (cambic horizon).

Microchemical analyses of selected features on the Bi horizon of the P₆ revealed a Si-rich micromass (30.10 % SiO₂ and 8.20 % Al₂O₃) with high contents of MgO and Fe₂O₃, surrounding quartz grains, Ti minerals, ferruginous sand-sized lithorelicts with 54.50 % of Fe₂O₃ and volcanic glass rich in Si and Ca (Table 7; Figure 10a). In addition, there are abundant grains of apatite, partially weathered wherein Ca is progressively replaced by Al (Table 7; Figure 10b). Illuvial coatings (ferrans and mangans) occur with variable composition (Table 7; Figures 10c and 10d). These secondary ferrans/mangans host high contents of Cu, Ni, Co, and P, with low levels of Si.

At the Bw₂ horizon of the Geric Rhodic Petroplinthic Ferralsol (P₇) many pedofeatures are typical of concretionary soils (Figures 11a and 11b). Alteromorphs with varying degrees of nuclear preservation are observed with secondary Fe cementation as nodules or concretions. These concretions of various sizes and types may include alteromorphs of pelitic rocks, and quartz grains. Ferrans may be formed either by hematite or by goethite.

The microchemical analysis and backscatter images of the Bw₂ horizon in P₇ show sand-sized micronodules (approximately 1.0 mm diameter) with a dominant ferruginous composition (up to 49.40 % Fe₂O₃); whereas the external clay micromass shows lower values of Fe₂O₃ (24.90 %), associated with higher Al and lower P values (Table 8;

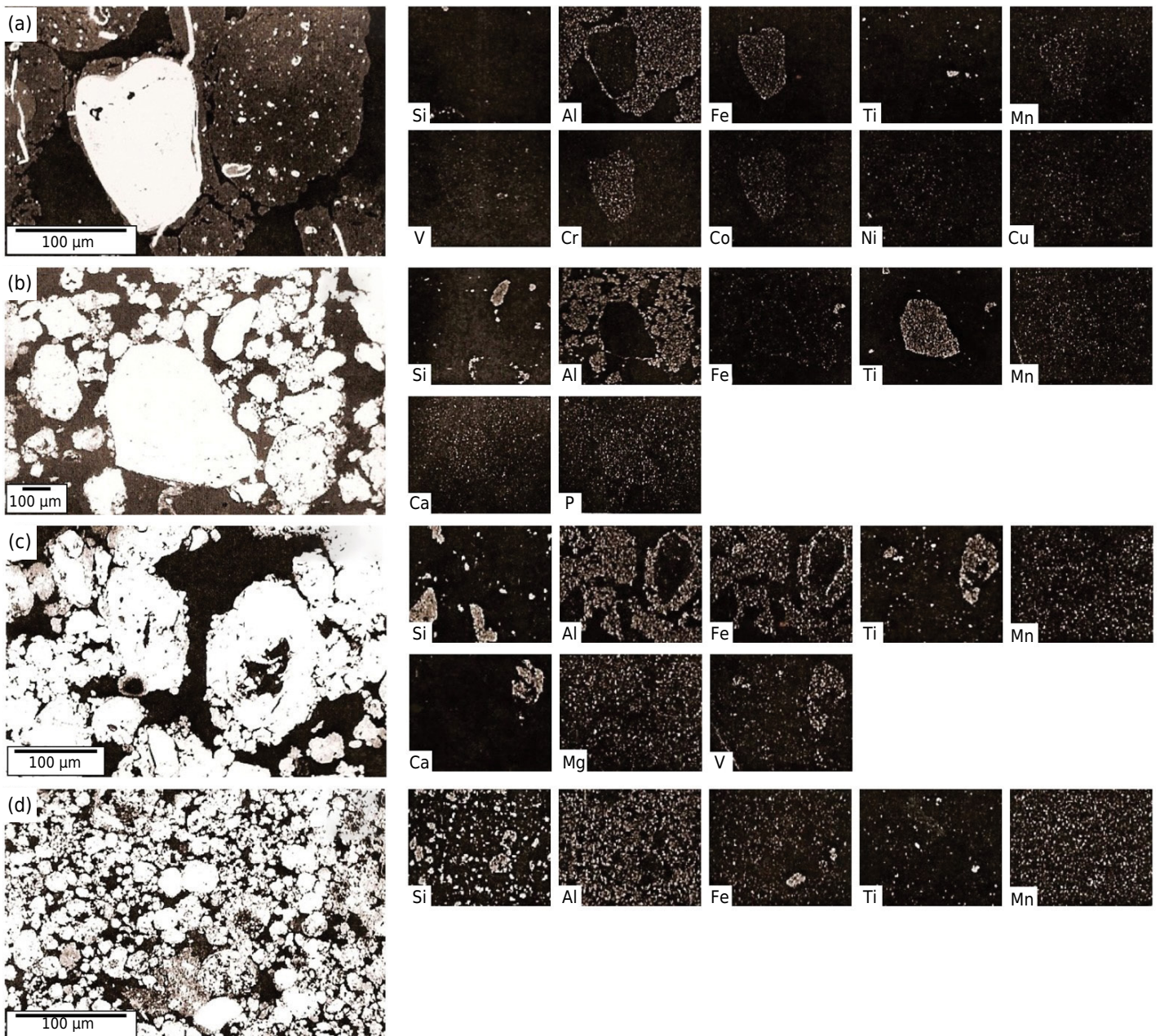


Figure 8. Scanning electron microscope photomicrographs and EDS microchemical maps of the Bw_2 horizon (a and b) in the P_4 - Geric Acric Gibbsic Ferralsol (Clayic, Dystric), and of the Bw_2 horizon (c and d) in the P_5 - Acric Rhodic Ferritic Ferralsol (Clayic, Dystric, Humic); Patrocínio topolithosequence. Fe/Cr-rich alteromorphs (a) and Ti minerals occurring as inclusions in the microaggregates (b), Ti-rich alteromorphs/perovskite (c), and Ti/Fe grains (d).

Figure 12a). This indicates a mixed kaolinitic-oxic nature of this soil. Some concretions and nodules have gibbsite inclusions (Al maps) with low levels of Fe and Si, and high aluminous composition (39.80 % Al_2O_3) (Table 8; Figure 12b). Phosphorous-rich grains with 14.30 % P_2O_5 associated to higher levels of Al, Fe, and Ti may also be observed (Table 8; Figure 12c).

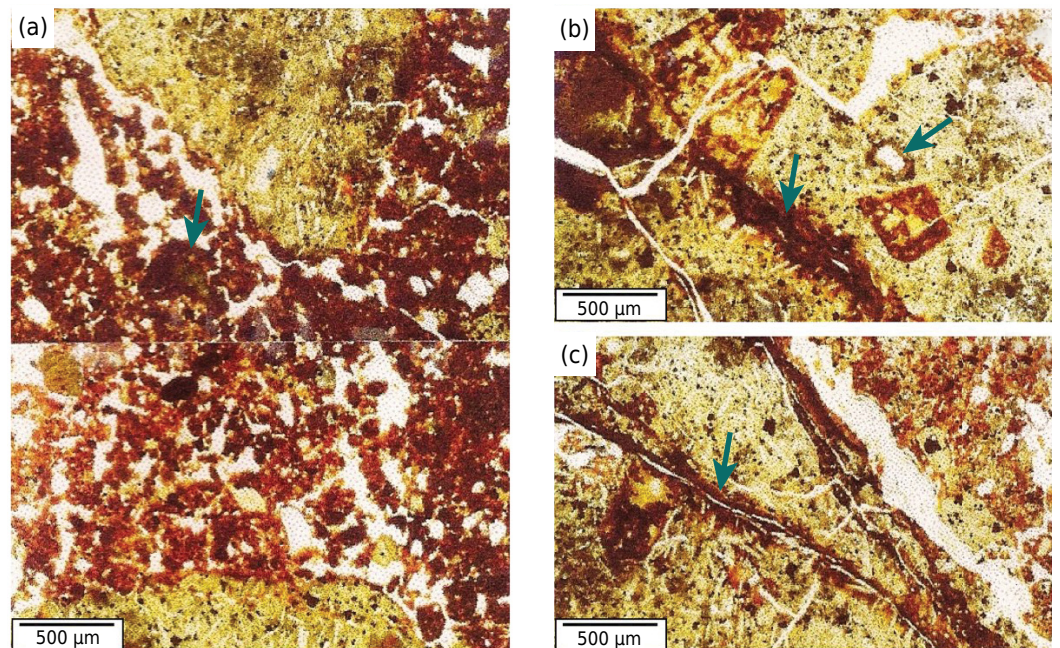
DISCUSSION

The strong microgranular structure of the Ferralsols with oxic composition is due to long-term pedobioturbation, as suggested by Schaefer (2001), Rückamp et al. (2012), Oliveira et al. (2014), and Stoops and Schaefer (2018). According to Stoops and Schaefer (2018), bioturbation is the main process contributing to the saprolite transformation onto

Table 6. SEM-WDS microchemical analysis of selected pedofeatures of the Bw₂ horizon in the P₅ - Acric Rhodic Ferritic Ferralsol (Clayic, Dystric, Humic); Patrocínio topolithosequence

Oxides	Perovskite grain	Ferruginous margin	Ferruginous nodule	Clay plasma	Biological channel (aggregate rich in organic matter)	Aggregate plasma	Ti-grain	External plasma
%								
MgO	0.20	0.35	4.43	0.19	1.10	0.51	0.16	0.42
Al ₂ O ₃	0.22	19.40	0.80	34.50	28.20	25.20	1.92	24.10
SiO ₂	0.19	1.25	0.27	10.50	9.20	7.90	0.37	7.80
P ₂ O ₅	0.18	0.25	0.12	0.54	0.40	0.47	0.65	0.50
K ₂ O	n.d.	n.d.	n.d.	n.d.	0.10	0.27	0.02	0.30
CaO	41.50	3.23	0.03	0.18	0.75	0.23	0.03	0.15
TiO ₂	49.10	28.40	40.10	4.10	2.70	4.25	59.10	4.15
Cr ₂ O ₃	n.d.	0.08	n.d.	n.d.	0.04	0.08	n.d.	0.10
MnO	n.d.	0.55	1.94	n.d.	0.08	0.05	0.08	0.06
Fe ₂ O ₃	0.61	35.30	30.70	25.30	20.10	20.40	8.90	21.30
CoO	0.10	0.24	0.30	0.28	n.d.	0.01	n.d.	0.02
NiO	0.13	0.07	0.08	0.15	n.d.	0.01	0.30	0.02
CuO	n.d.	n.d.	n.d.	n.d.	0.18	0.40	0.10	0.30
ZnO	0.16	0.02	0.01	n.d.	0.06	0.03	0.03	0.02
BaO	2.30	0.08	n.d.	n.d.	n.d.	n.d.	n.d.	n.d.
NbO	0.40	0.30	0.60	n.d.	n.d.	n.d.	0.60	n.d.
Ki ⁽¹⁾				0.52	0.55	0.53		0.55

⁽¹⁾ Weathering index (Ki) was only determined for micromass, in which $Ki = (SiO_2 \times 1.7)/Al_2O_3$; n.d.: not detected.


Figure 9. Photomicrographs of the Bi horizon in the P₆ - Eutric Chromic Petroplintic Leptic Cambisol (Clayic, Humic); Coromandel topolithosequence. Arrows indicate well-developed granular structure (a), and mangans and ferrans commonly found along pores, and coating grains (b and c).

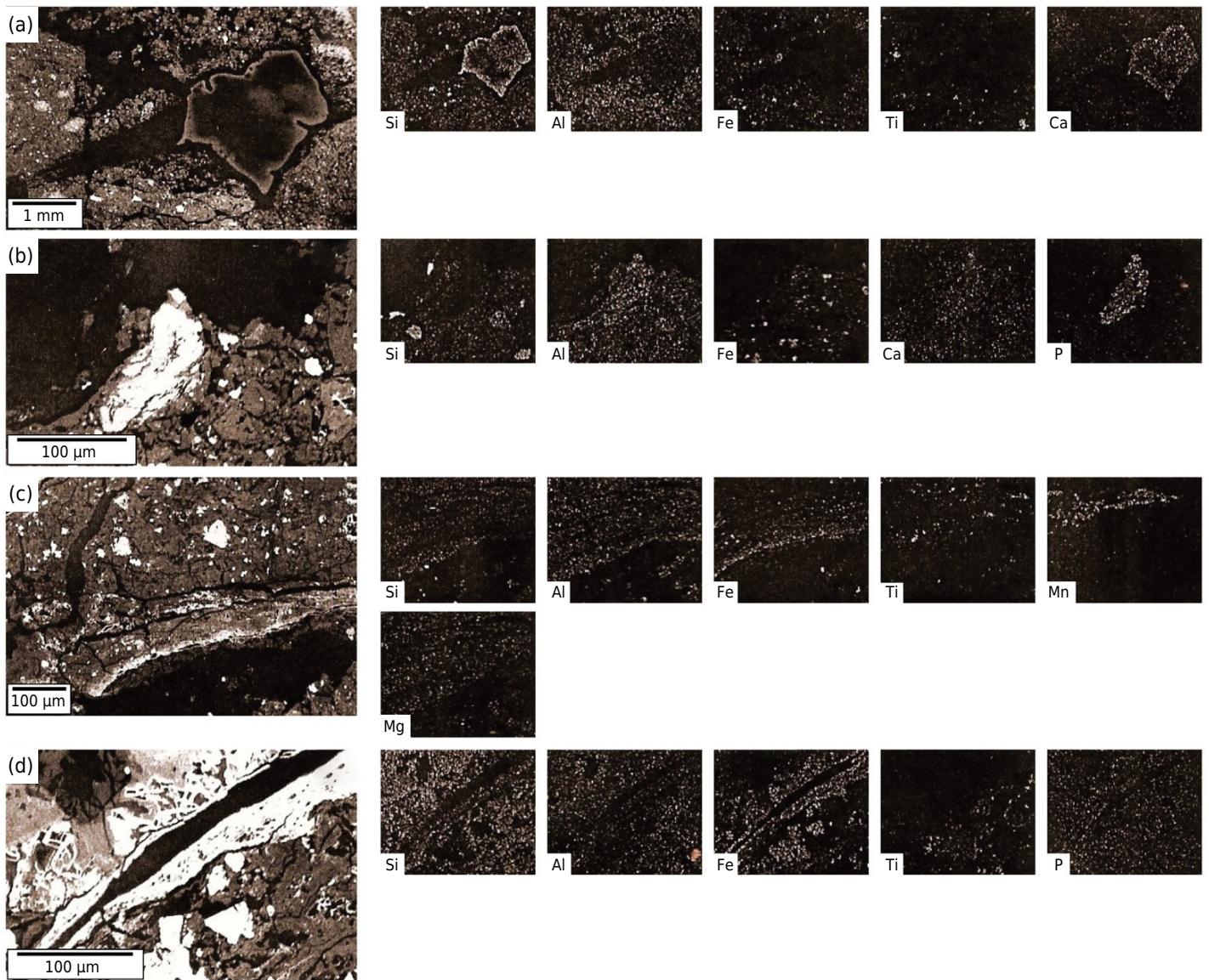


Figure 10. Scanning electron microscope photomicrographs and EDS microchemical maps of the Bi horizon in the P₆ - Eutric Chromic Petrolintic Leptic Cambisol (Clayic, Humic); Coromandel topolithosequence. Volcanic glass rich in Si and Ca (a), apatite grains partially weathered (b), and illuvial coatings (ferrans and mangans) (c and d).

a stable, homogeneous microstructure, particularly by termite activity (Martins, 2007; Kooistra and Pulleman, 2018).

The mineral assemblage of the Cambisol (P₂) indicates a contribution of allochthonous metapelitic rocks, of nearby Bambuí Group, besides the local alkaline igneous rock, showing a polycyclic nature and mixing. The cambic horizon (P₂ - Bi) is typically shallow, with preserved grains of primary minerals, but structurally resembles a Ferralsol, similarly to Ferralsol-Cambisols intergrade from elsewhere in Brazil (Albuquerque Filho et al., 2008).

The microgranular structure of cambic horizons indicates intense pedobiological activity at present times, superimposed on pre-weathered materials (Miklós, 1992; Schaefer, 2001) with an abrupt, short-range pedoplasation zone (Stoops and Schaefer, 2018; Schaefer, 2018), corroborating the morphological field observations. Other pedofeatures are altered Ti minerals, ferruginous nodules, and apatite inclusions (Figure 4a). This indicates that Cambisols may change directly to Ferralsols simply by increasing depth since either 0.50 m for Brazilian Soil Classification System (Santos et al., 2018) or 0.30 m

Table 7. SEM-WDS microchemical analysis of selected pedofeatures of the Bi horizon in the P₆ - Eutric Chromic Petroplinthic Leptic Cambisol (Clayic, Humic); Coromandel topolithosequence

Oxides	Ferruginous lithorelics	External plasma	Volcanic glass Si/Ca	Nodule Ca/P	Mangans	Ferrans
%						
MgO	0.09	3.10	2.60	1.55	0.80	1.90
Al ₂ O ₃	2.72	8.20	1.60	12.80	3.10	11.70
SiO ₂	2.68	30.10	44.40	2.65	5.90	2.40
P ₂ O ₅	n.d.	0.05	n.d.	12.20	1.60	0.36
K ₂ O	0.02	10.10	n.d.	1.28	1.20	0.03
CaO	0.06	0.16	8.20	1.98	0.10	0.20
TiO ₂	0.25	1.60	n.d.	1.77	1.05	0.60
VO ₂	0.30	0.04	0.08	n.d.	0.40	0.04
CrO	0.35	0.10	n.d.	n.d.	n.d.	n.d.
MnO	n.d.	0.06	n.d.	n.d.	32.80	0.40
Fe ₂ O ₃	54.50	18.80	0.04	12.60	15.20	53.90
CoO	0.08	0.28	0.07	n.d.	0.85	0.55
NiO	0.06	0.06	0.05	n.d.	0.65	0.02
CuO	n.d.	0.06	n.d.	0.09	0.63	0.50
ZnO	n.d.	0.04	n.d.	n.d.	n.d.	n.d.
Ki ⁽¹⁾		6.24			3.24	0.35

⁽¹⁾ Weathering index (Ki) was only determined for micromass, in which $Ki = (SiO_2 \times 1.7)/Al_2O_3$; n.d.: not detected.

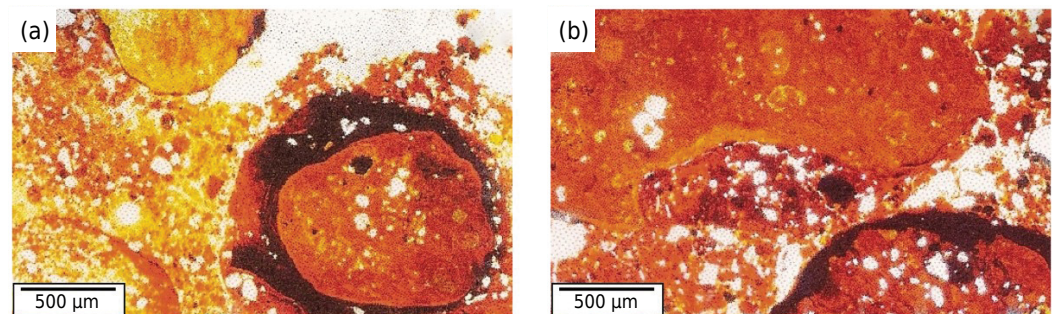


Figure 11. Photomicrographs of the Bw₂ horizon in the P₇ - Geric Rhodic Petroplinthic Ferralsol (Clayic, Dystric); Coromandel topolithosequence. Ferruginous concretions including quartz grains, and with ferrans formed either by hematite or by goethite (a and b).

for Soil Taxonomy (Soil Survey Staff, 1999) are the minimum thickness for oxic horizons. This is consistent with previous Cambisol-Ferralsol transitions reported in Brazil (Muggler and Buurman, 1997; Schaefer, 2018).

The amounts of P₂O₅ in the clay micromass surrounding the apatite grain indicates P dissolution with further strong adsorption by clays, corroborated by results of Rolim Neto et al. (2004) and Schaefer et al. (2008). The micromass with larger illite/smectite aggregates (Ki = 2.84) and higher K, Mg and Fe values, supports the high nutrient status observed in these Cambisols (Table 3), corroborating a low weathering degree.

The micromass surrounding the Ti grains and concretions is typically oxic and aluminous, with varying amounts of Fe (12.20 - 14.40 % Fe₂O₃), and high Ti (2.60 - 4.10 % TiO₂), mostly anatase, finely dispersed in the micromass (Table 4). Since the isoelectric

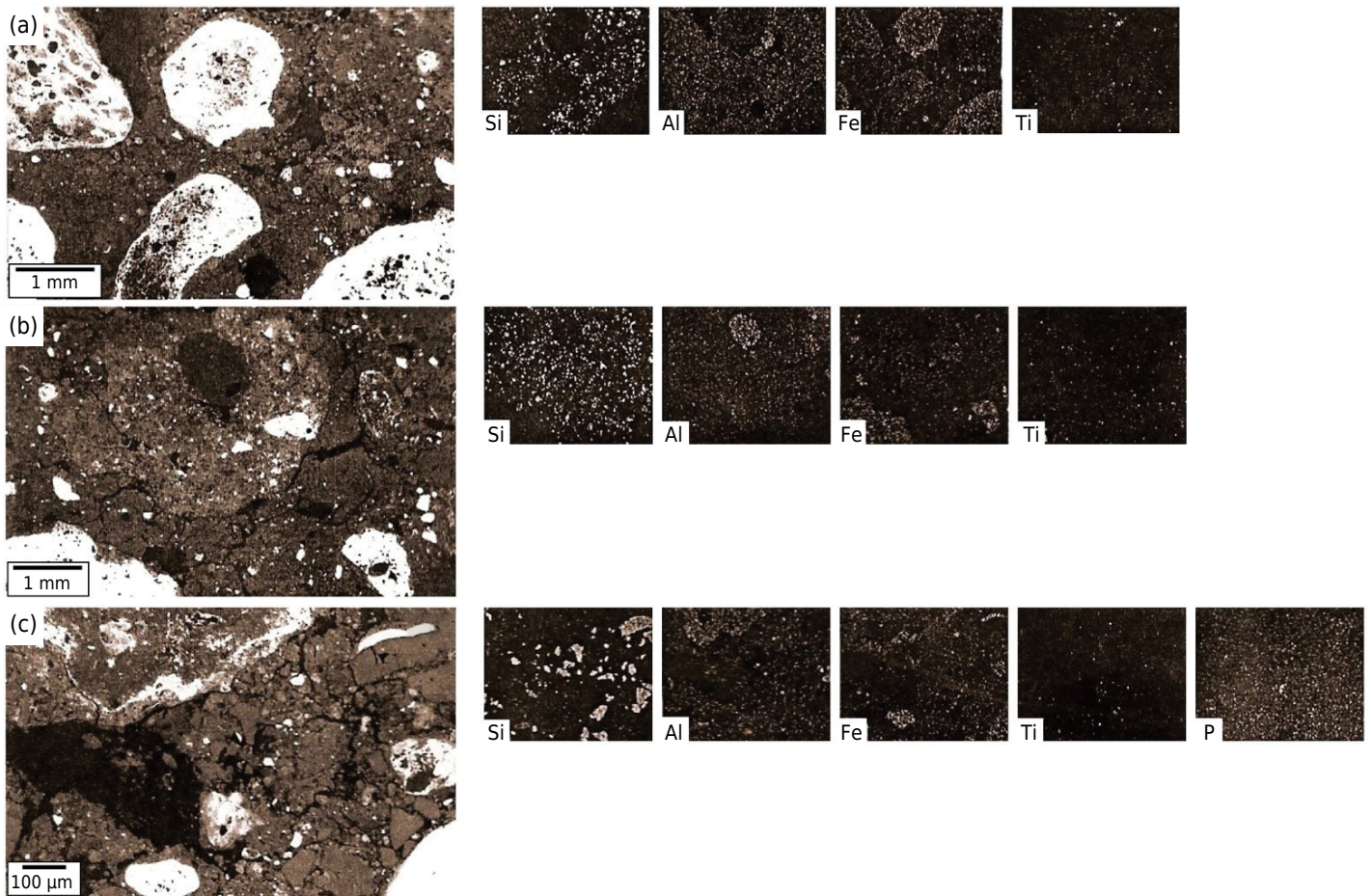


Figure 12. SEM photomicrographs and EDS microchemical maps of the Bw₂ horizon in the P₇ - Geric Rhodic Petroplinthic Ferralsol (Clayic, Dystric); Coromandel topolithosequence. Sand-sized micronodules (a and b), and quartz and P-rich grains (c).

Table 8. SEM-WDS microchemical analysis of selected pedofeatures of the Bw₂ horizon in the P₇ - Geric Rhodic Petroplinthic Ferralsol (Clayic, Dystric); Coromandel topolithosequence

Oxides	Ferruginous concretion	External plasma to Fe concretion	Gibbsite grains	Al-phosphatic nodule	External plasma to the Al-phosphatic nodule
MgO	1.25	0.51	0.08	0.08	0.42
Al ₂ O ₃	2.20	19.50	39.80	18.80	18.10
SiO ₂	1.60	15.50	1.90	3.20	17.20
P ₂ O ₅	0.50	0.05	1.20	14.30	0.05
K ₂ O	0.05	0.45	0.05	0.05	0.30
CaO	0.20	0.10	0.10	0.60	0.10
TiO ₂	1.20	2.25	0.08	1.85	2.72
CrO	0.06	0.10	n.d.	n.d.	0.12
MnO	0.28	0.10	n.d.	0.10	0.10
Fe ₂ O ₃	49.40	24.90	0.80	6.50	23.60
CoO	0.65	n.d.	n.d.	0.24	0.15
CuO	0.55	0.05	n.d.	n.d.	0.01
MoO	n.d.	n.d.	n.d.	2.20	n.d.
Ki ⁽¹⁾		1.35			1.62

⁽¹⁾ Weathering index (Ki) was only determined for micromass, in which $Ki = (SiO_2 \times 1.7)/Al_2O_3$; n.d.: not detected.

point of Ti minerals is relatively high (rutile = 5.3; anatase = 6.2), their influence in P adsorption can be considerable in such soils from ultramafic rocks. The presence of leucoxene, typical of lower metamorphic grade lithologies (Milnes and Fitzpatrick, 1989), confirms the mixture of different materials, with the contribution of metapelitic rocks of the Bambuí Group.

Although the Perovskite may represent a considerable and surprising Ca reserve in Ferralsols (P₅ Ferralsol, for example), and an unusual feature for deeply weathered soils, its presence indicates an extreme resistance to weathering and dissolution, not yet reported in the literature (Jackson, 1964; Milnes and Fitzpatrick, 1989). In this regard, the presence of up to 8 % of perovskite in ultrabasic/alkaline rocks (Williams et al., 1970) and in alkaline-ultrabasic tuffs (Barbosa et al., 1970) of Upper Paranaíba volcanic province, corroborates the importance of this mineral to deeply weathered soils of this region.

The presence of leucoxene grains within aggregates shows that intense, long-term pedobioturbation account for the incorporation of these resistant residual minerals, with varying chemical composition in these polygenetic deep-weathered soils. Besides leucoxene, allochthonous quartz grains and charcoal fragments are found in aggregates, as described by Schaefer (2001) and Schaefer et al. (2008) in Ferralsols elsewhere from Brazil.

The presence of residual magnetite grains in Ferralsols (P₇) (dark opaques) suggests an intimate admixture of volcanic materials with metapelitic (Bambuí Group), probably as mixed colluvial deposits, similar to colluvial soils on phyllites, described by Muggler and Buurman (1997).

There is a common presence of altered apatite inclusions (diameter ≤ 10 mm), associated with ulvospinel mineral and ilmenite, all highly resistant to weathering, as shown by Cescas et al. (1970). In this regard, Camêlo et al. (2015) also reported the highest P and Ca contents for B horizons of Ferralsols originating from ultramafic tuffites of the Upper Paranaíba region. However, P forms included in Ti/Fe minerals have very low solubility, and are unlikely to represent a potential P-reserve for annual crops in the short term.

CONCLUSIONS

Ferralsols of the Brazilian Central Plateau are polygenetic, and the chemical composition of discrete mineral grains at high magnification allowed to distinguish between ultramafic and metapelitic parent materials.

The advanced well-formed oxic microstructure of these Ferralsols is due to long-term pedobioturbation, in which resistant primary minerals are randomly incorporated within the homogeneous oxic, acric (gibbsite/Fe-oxides rich) micromass inherited from the saprolite. Charcoal and allochthonous quartz grains, side-by-side with ultrabasic-related Ti-magnetite and perovskite, all randomly incorporated within the aggregates, indicate a polycyclic genesis of these soils.

Shallow soils on slopes with cambic horizons, also displayed an unusual microgranular structure, favored by intense biological activity and consistent with current tropical climate. They are formed on tuffites, and secondary clay minerals are a mix of expandable 2:1 clays (nontronite), with Fe oxides and kaolinite; therefore, with a lower weathering degree when compared to the Ferralsols, despite the microgranular structure.

The Cambisols developed from tuffite (volcanic tuffs) and ultrabasic rocks on slopes have apatite as residual grains, associated with Ca, Fe, and K-rich minerals, indicating a polygenetic colluvial mixture of volcanic and pelitic materials.

The widespread occurrence of perovskite (CaTiO_3) as residual grains even in the most weathered Ferralsols, indicates an unusual and unreported Ca reserve associated with titaniferous minerals still unknown in acric Ferralsols of Central Brazil.

ACKNOWLEDGMENTS

The authors acknowledge the Federal University of Viçosa for the infrastructure for the development of this work, the Coordination for the Improvement of Higher Level Personnel (Capes) and the National Council for Scientific and Technological Development (CNPq) for the financial support, and the Universidade Federal Rural de Pernambuco.

AUTHOR CONTRIBUTIONS

Conceptualization: Fernando Cartaxo Rolim Neto and Carlos Ernesto Gonçalves Reynaud Schaefer.

Methodology: Fernando Cartaxo Rolim Neto.

Validation: Carlos Ernesto Gonçalves Reynaud Schaefer, Danilo de Lima Camêlo, Marcelo Metri Corrêa, and Roberto da Boa Viagem Parahyba.

Formal Analysis: Carlos Ernesto Gonçalves Reynaud Schaefer, Danilo de Lima Camêlo, Marcelo Metri Corrêa, and Roberto da Boa Viagem Parahyba.

Investigation: Fernando Cartaxo Rolim Neto.

Data Curation: Fernando Cartaxo Rolim Neto.

Writing - Original Draft: Fernando Cartaxo Rolim Neto.

Writing - Review and Editing: Carlos Ernesto Gonçalves Reynaud Schaefer, Danilo de Lima Camêlo, Marcelo Metri Corrêa, Roberto da Boa Viagem Parahyba, Anildo Monteiro Caldas, and Anifo Soares Mamudo Ibraimo.

Visualization: Anildo Monteiro Caldas and Anifo Soares Mamudo Ibraimo.

Supervision: Carlos Ernesto Gonçalves Reynaud Schaefer.

Project Administration: Carlos Ernesto Gonçalves Reynaud Schaefer.

Funding Acquisition: Carlos Ernesto Gonçalves Reynaud Schaefer.

REFERENCES

- Albuquerque Filho MR, Muggler CC, Schaefer CEGR, Ker JK, Santos FC. Solos com morfologia latossólica e caráter câmbico na região de Governador Valadares, Médio Rio Doce, Minas Gerais: gênese e micromorfologia. *Rev Bras Cienc Solo*. 2008;32:259-70. <https://doi.org/10.1590/S0100-06832008000100025>
- Alvares CA, Stape JL, Sentelhas PC, Gonçalves JLM, Sparovek G. Köppen's climate classification map for Brazil. *Meteorol Z*. 2013;22:711-28. <https://doi.org/10.1127/0941-2948/2013/0507>
- Baert J, van Ranst E. Comparative micromorphological study of representative weathering profiles on different parent materials in the lower Zaire. In: Shoba S, Gerasimova M, Miedema R, editors. *Proceedings of the X International working meeting on soil micromorphology. Soil micromorphology: studies on soil diversity diagnostics dynamics*. Wageningen: Moscow - Wageningen; 1997. p. 28-40.
- Barbosa O, Braun OPG, Dyer RC, Cunha CABR. *Geologia da região do Triângulo Mineiro*. Rio de Janeiro: DNPM, Divisão de Fomento da Produção Mineral; 1970. (Boletim 136).

- Bullock P, Fedoroff N, Jongerius A, Stoops G, Tursina T, Babel U. Handbook for soil thin section description. Wolverhampton: Waine Research; 1985.
- Camêlo DL, Ker JC, Fontes MPF, Corrêa MM, Costa ACS, Melo VF. Pedogenic iron oxides in iron-rich Oxisols developed from mafic rocks. *Rev Bras Cienc Solo*. 2017;41:e0160379. <https://doi.org/10.1590/18069657rbc20160379>
- Camêlo DL, Ker JC, Fontes MPF, Costa ACS, Corrêa MM, Leopold M. Mineralogy, magnetic susceptibility and geochemistry of Fe-rich Oxisols developed from several parent materials. *Sci Agric*. 2018;75:410-9. <https://doi.org/10.1590/1678-992x-2017-0087>
- Camêlo DL, Ker JC, Novais RF, Corrêa MM, Lima VC. Sequential extraction of phosphorus by Mehlich-1 and ion exchange resin from B horizons of Ferric and Perferic Latosols (Oxisols). *Rev Bras Cienc Solo*. 2015;39:1058-67. <https://doi.org/10.1590/01000683rbc20140405>
- Carmo DN, Curi N, Resende M. Caracterização e gênese de Latossolos da Região do Alto Paranaíba - MG. *Rev Bras Cienc Solo*. 1984;8:235-40.
- Cescas MP, Týner EH, Syers JK. Distribution of apatite and other mineral inclusions in a rhyolitic pumice ash and beach sands from New Zealand: an electron-microprobe study. *Eur J Soil Sci*. 1970;21:78-84. <https://doi.org/10.1111/j.1365-2389.1970.tb01154.x>
- Delvigne JE. Atlas of micromorphology and mineralogy. Ottawa: Orstom; 1998. (Special Publication 3).
- Duarte MN, Ramos DP, Lima PC. Caracterização e gênese de solos desenvolvidos de cobertura quaternária sobre embasamento cristalino na Baixada Litorânea do Estado do Rio de Janeiro. *Rev Bras Cienc Solo*. 1996;20:291-304.
- Ferreira SAD, Santana DP, Fabris JD, Curi N, Nunes Filho E, Coey JMD. Relações entre magnetização, elementos traços e litologia de duas seqüências de solos do estado de Minas Gerais. *Rev Bras Cienc Solo*. 1994;18:167-74.
- IUSS Working Group WRB. World reference base for soil resources 2014, update 2015: International soil classification system for naming soils and creating legends for soil maps. Rome: Food and Agriculture Organization of the United Nations; 2015. (World Soil Resources Reports, 106).
- Jackson JA, Bates RL. Glossary of geology. 4th ed. Falls Church: American Geological Institute; 1997.
- Jackson ML. Chemical composition of soils. In: Bear FE, editor. *Chemistry of the soil*. 2nd ed. New York: Van Nostrand Reinhold Company; 1964. p. 71-141.
- Ker JC. Latossolos do Brasil: uma revisão. *Geonomos*. 1997;5:17-40. <https://doi.org/10.18285/geonomos.v5i1.187>
- Kooistra MJ, Pulleman MM. Features related to faunal activity. In: Stoops G, Marcelino V, Mees F, editors. *Interpretation of micromorphological features of soils and regoliths*. 2nd ed. Amsterdam: Elsevier; 2018. p. 447-70.
- Marcelino V, Schaefer CEGR, Stoops G. Oxic and related materials. In: Stoops G, Marcelino V, Mees F, editors. *Interpretation of micromorphological features of soils and regoliths*. 2nd ed. Amsterdam: Elsevier; 2018. p. 663-90.
- Marques JJGSM. Trace elements distribution in Brazilian cerrado soils at the landscape and micrometer scales [thesis]. West Laffayette: Purdue University; 2000.
- Martins GM. Efeitos da ação de cupins sobre propriedades de um perfil de solo em uma vertentete da represa Billings - São Bernado do Campo/SP [dissertação]. São Paulo: Universidade de São Paulo; 2007.
- Miklós AAW. Biodynamique d'une couverture pédologique dans la région de Botucatu, Brésil [thesis]. France: Université Paris VI; 1992.
- Milnes AR, Fitzpatrick RW. Titanium and zirconium minerals. In: Dixon JB, Weed SB, editors. *Minerals in soil environments*. 2nd ed. Madison: Soil Science Society of America; 1989. p. 1131-94.

- Muggler CC, Buurman P. Micromorphological aspects of polygenetic soils developed on phyllitic rocks in Minas Gerais, Brazil. In: Shoba S, Gerasimova M, Miedema R, editors. Proceedings of the X International working meeting on soil micromorphology. Soil micromorphology: studies on soil diversity diagnostics dynamics. Wageningen: Moscow - Wageningen; 1997. p. 129-38.
- Nunes WAGA, Schaefer CEGR, Ker JC, Fernandes Filho EI. Caracterização micropedológica de alguns solos da Zona da Mata Mineira. *Rev Bras Cienc Solo*. 2000;24:103-15. <https://doi.org/10.1590/S0100-0683200000100013>
- Oliveira FS, Varajão AFDC, Varajão CAC, Schaefer CEGR, Boulangé B. The role of biological agents in the microstructural and mineralogical transformations in aluminium lateritic deposit in Central Brazil. *Geoderma*. 2014;226-227:250-9. <https://doi.org/10.1016/j.geoderma.2014.02.012>
- Paisani JC, Pontelli ME, Corrêa ACB, Rodrigues RAR. Pedogeochemistry and micromorphology of Oxisols – a basis for understanding etchplanation in the Araucárias Plateau (Southern Brazil) in the Late Quaternary. *J S Am Earth Sci*. 2013;48:1-12. <https://doi.org/10.1016/j.jsames.2013.07.011>
- Rolim Neto FC, Schaefer CEGR, Costa LM, Corrêa MM, Fernandes Filho EI, Ibraimo MM. Adsorção de fósforo, superfície específica e atributos mineralógicos em solos desenvolvidos de rochas vulcânicas do Alto Paranaíba (MG). *Rev Bras Cienc Solo*. 2004;28:953-64. <https://doi.org/10.1590/S0100-06832004000600003>
- Rolim Neto FC, Schaefer CEGR, Fernandes Filho EI, Corrêa MM, Costa LM, Parahyba RBV, Guerra SMS, Heck R. Topolitosequências de solos de Alto Paranaíba: atributos físicos, químicos e mineralógicos. *Rev Bras Cienc Solo*. 2009;33:1795-809. <https://doi.org/10.1590/S0100-06832009000600028>
- Rückamp D, Martius C, Bornemann L, Kurzatkowski D, Naval LP, Amelung W. Soil genesis and heterogeneity of phosphorus forms and carbon below mounds inhabited by primary and secondary termites. *Geoderma*. 2012;170:239-50. <https://doi.org/10.1016/j.geoderma.2011.10.004>
- Santos HG, Jacomine PKT, Anjos LHC, Oliveira VA, Lumbreras JF, Coelho MR, Almeida JA, Araújo Filho JC, Oliveira JB, Cunha TJF. Sistema brasileiro de classificação de solos. 5. ed. rev. ampl. Brasília, DF: Embrapa; 2018.
- Schaefer CEGR. Brazilian highland soils and Oxisols from deep weathered saprolites. In: 21st World Congress of Soil Science; August 2018; Rio de Janeiro. Rio de Janeiro: Sociedade Brasileira de Ciência do Solo; 2018.
- Schaefer CEGR. Brazilian Latosols and their B horizon microstructure as long-term biotic constructs. *Aust J Soil Res*. 2001;39:909-26. <https://doi.org/10.1071/SR00093>
- Schaefer CEGR, Fabris JD, Ker JC. Minerals in the clay fraction of Brazilian Latosols (Oxisols): a review. *Clay Miner*. 2008;43:137-54. <https://doi.org/10.1180/claymin.2008.043.1.11>
- Schaefer CEGR, Ker JC, Gilkes RJ, Campos JC, Costa LM, Saadi A. Pedogenesis on the uplands of the Diamantina Plateau, Minas Gerais, Brazil: a chemical and micropedological study. *Geoderma*. 2002;107:243-69. [https://doi.org/10.1016/S0016-7061\(01\)00151-3](https://doi.org/10.1016/S0016-7061(01)00151-3)
- Soil Survey Staff. Soil taxonomy: a basic system of soil classification for making and interpreting soil surveys. 2nd ed. Washington, DC: United States Department of Agriculture, Natural Resources Conservation Service; 1999. (Agricultural Handbook, 436).
- Stoops G. Guidelines for the analysis and description of soil and regolith thin sections. Madison: Soil Science Society of America; 2003.
- Stoops GJ, Buol SW. Micromorphology of Oxisols. In: Douglas LA, Thompson ML, editors. Soil micromorphology and soil classification. Madison: Soil Science Society of America; 1985. p. 105-19.
- Stoops G, Marcelino V, Mees F, editors. Interpretation of micromorphological features of soils and regoliths. 2nd ed. Amsterdam: Elsevier; 2018.

- Stoops G, Marcelino V, Zauyah S, A Maas. Micromorphology of soils in humid tropics. In: Ringrose-Voase AJ, Humphreys GS, editors. Soil micromorphology: studies in management and genesis. Amsterdam: Elsevier; 1993. p. 1-15.
- Stoops G, Schaefer CEGR. Pedoplasmatation: formation of soil material. In: Stoops G, Marcelino V, Mees F, editors. Interpretation of micromorphological features of soils and regoliths. 2nd ed. Amsterdam: Elsevier; 2018. p. 59-72.
- Tardy Y, Roquin C. Geochemistry and evolution of lateritic landscapes. In: Martin, IP, Chesworth W, editors. Weathering, soils and paleosols. Amsterdam: Elsevier; 1992. p. 407-44.
- Thomas MF. Geomorphology in the tropics: a study of weathering and denudation at low latitudes. New York: John Wiley & Sons; 1994.
- Williams HFJ, Turner FJ, Gilbert CM. Petrografia: uma introdução ao estudo das rochas em seções delgadas. São Paulo: USP; 1970.